Integrated Hydrogenated Amorphous Si Photodiode Detector for Microfluidic Bioanalytical Devices

ARTICLE *in* ANALYTICAL CHEMISTRY · NOVEMBER 2003

Impact Factor: 5.64 · DOI: 10.1021/ac0301550 · Source: PubMed

6 AUTHORS, INCLUDING:

Toshihiro Kamei
University of California, Berkeley
51 PUBLICATIONS **591** CITATIONS

SEE PROFILE

James R Scherer
University of California, Berkeley
59 PUBLICATIONS **2,681** CITATIONS

SEE PROFILE

Alison M Skelley
microFluent
38 PUBLICATIONS **1,331** CITATIONS

SEE PROFILE

Anal. Chem. **2003,** *75,* 5300−5305

Articles

Integrated Hydrogenated Amorphous Si Photodiode Detector for Microfluidic Bioanalytical Devices

Toshihiro Kamei,[†,§] Brian M. Paegel,[†] James R. Scherer,[†] Alison M. Skelley,[†] Robert A. Street,[‡] and Richard A. Mathies*[,†]

Department of Chemistry, University of California, Berkeley, California 94720, and Palo Alto Research Center, Palo Alto, California 94304

Hydrogenated amorphous silicon (a-Si:H) PIN photodiodes have been developed and characterized as fluorescence detectors for microfluidic analysis devices. A discrete a-Si:H photodiode is first fabricated on a glass substrate and used to detect fluorescent dye standards using conventional confocal microscopy. In this format, the limit of detection for fluorescein flowing in a 50-μm deep channel is 680 pM ($S/N = 3$). A hybrid integrated detection system consisting of a half-ball lens, a ZnS/YF_3 multilayer optical interference filter with a pinhole, and an annular a-Si:H photodiode is also developed that allows the laser excitation to pass up through the central aperture in the detector. Using this integrated detection device, the limit of detection for fluorescein is 17 nM, and DNA fragment sizing and chiral analysis of glutamic acid are successfully performed. The a-Si:H detector exhibits high sensitivity at the emission wavelengths of commonly used fluorescent dyes and is readily microfabricated and integrated at low cost making it ideal for portable microfluidic bioanalyzers and emerging large scale integrated microfluidic technologies.

Microfabrication technology is profoundly influencing the development of modern analytical devices in chemistry and biology.[1] Micrometer-scale geometric definition afforded by photolithographic patterning makes possible the precise manipulation of nano- and picoliter quantities of sample and the fabrication of microfluidic capillary electrophoresis (CE) systems with dramatically reduced analysis times. Microfluidic CE device versatility has manifested itself in applications as diverse as DNA fragment sizing,[2] DNA sequencing,[3] immunoassay,[4] amino acid analysis,[5] and protein analysis.[6] Furthermore, microfabrication technology has facilitated the production of high-throughput 96- and 384-channel microfluidic CE devices.[7,8] The next frontier for lab-on-a-chip devices is achieving a higher degree of automation by integrating all of the steps and components for an analysis process within or on the microfluidic device.

A variety of approaches toward the goal of more complete process integration have been presented. Microfluidic valves and pumps[9] have been developed for highly parallel fluid handling in the silicone elastomer poly(dimethylsiloxane) (PDMS) by using soft lithography,[10] and they have been used to perform cell sorting[11] and combinatorial optimization of protein crystallization.[12] Methods for fabricating high-density arrays of membrane valves and pumps in glass microfluidic structures have been presented[13] that are particularly useful when chemical compatibility and high sensitivity detection are required. Microfluidic sample preparation process technologies have been developed, including PCR coupled with high-speed electrophoresis,[14−16] nanovolume DNA sequencing process chemistries,[17] and integrated genetic assays.[18, 19]

Despite this miniaturization and large-scale integration of fluid handling and biochemical assays, high-sensitivity microfluidic

* Corresponding author. Phone: (510)642-4192. Fax: (510)642-3599. E-mail: rich@zinc.cchem.berkeley.edu.

[†] University of California.

[‡] Palo Alto Research Center.

[§] On leave from National Institute of Advanced Industrial Science and Technology (AIST), Tsukuba, Ibaraki, 305-8568, Japan.

(1) *Micro Total Analysis Systems 2002*; Baba, Y., Shoji, S., van den Berg, A., Eds.; Kluwer Academic Publishers: Dordrecht, 2002.

(2) Woolley, A. T.; Mathies, R. A. *Proc. Natl. Acad. Sci. U.S.A.* **1994**, *91*, 11348−11352.

(3) Woolley, A. T.; Mathies, R. A. *Anal. Chem.* **1995**, *67*, 3676−3680.

(4) Chiem, N.; Harrison, D. J. *Anal. Chem.* **1997**, *69*, 373−378.

(5) Harrison, D. J.; Fluri, K.; Seiler, K.; Fan, Z. H.; Effenhauser, C. S.; Manz, A. *Science* **1993**, *261*, 895−897.

(6) Yao, S.; Anex, D. S.; Caldwell, W. B.; Arnold, D. W.; Smith, K. B.; Schultz, P. G. *Proc. Natl. Acad. Sci. U.S.A.* **1999**, *96*, 5372−5377.

(7) Shi, Y.; Simpson, P. C.; Scherer, J. R.; Wexler, D.; Skibola, C.; Smith, M. T.; Mathies, R. A. *Anal. Chem.* **1999**, *71*, 5354−5361.

(8) Emrich, C. A.; Tian, H. J.; Medintz, I. L.; Mathies, R. A. *Anal. Chem.* **2002**, *74*, 5076−5083.

(9) Unger, M. A.; Chou, H. P.; Thorsen, T.; Scherer, A.; Quake, S. R. *Science* **2000**, *288*, 113−116.

(10) Xia, Y. N.; Whitesides, G. M. *Annu. Rev. Mater. Sci.* **1998**, *28*, 153−184.

(11) Fu, A. Y.; Chou, H. P.; Spence, C.; Arnold, F. H.; Quake, S. R. *Anal. Chem.* **2002**, *74*, 2451−2457.

(12) Hansen, C. L.; Skordalakes, E.; Berger, J. M.; Quake, S. R. *Proc. Natl. Acad. Sci. U.S.A.* **2002**, *99*, 16531−16536.

(13) Grover, W. H.; Skelley, A. M.; Liu, C. N.; Lagally, E. T.; Mathies, R. A. *Sens. Actuators, B* **2003**, *89*, 315−323.

(14) Woolley, A. T.; Hadley, D.; Landre, P.; deMello, A. J.; Mathies, R. A.; Northrup, M. A. *Anal. Chem.* **1996**, *68*, 4081−4086.

(15) Lagally, E. T.; Simpson, P. C.; Mathies, R. A. *Sens. Actuators, B* **2000**, *63*, 138−146.

10.1021/ac0301550 CCC: $25.00
Published on Web 09/11/2003

analysis still typically requires fluorescence detection systems that are comprised of large lasers, optical systems, and detectors. To access the potential portability of microfluidic analysis systems, the fluorescence detection system must also be miniaturized and integrated. Toward this end, in one effort a photoresist microlens was microfabricated on a microfluidic chip, but discrete external detectors were used.[20] A microavalanche Si photodiode (μAPD) has been embedded in a PDMS microfluidic device and used to detect separations of proteins and small molecules.[21] A miniaturized spectrometer using either a micromachined grating and CMOS imager[22] or a filtered crystalline silicon (c-Si) detector array was also presented.[23] Finally, a microfluidic system has also been integrated by depositing parylene-C over a c-Si photodiode.[24] While much progress has been made toward a miniaturized integrated detection system, the c-Si photodiode fabrication typically employed requires high process temperatures (~1000 °C), rendering it more difficult to integrate directly with glass- or plastic-based microfluidics.

Hydrogenated amorphous silicon (a-Si:H) is a valuable phototransducer material because it can be deposited at low temperatures (~200 °C) by using plasma-enhanced chemical vapor deposition (PECVD), and in situ impurity doping can be performed by adding impurity gases such as B_2H_6 and PH_3 into the SiH_4 source gas during growth.[25] These attributes permit the direct fabrication of an a-Si:H photodiode on inexpensive glass and plastic substrates. The absorption coefficient of c-Si, an indirect band gap semiconductor, is low due to momentum conservation for electronic transitions.[26] The disordered structure of a-Si:H, however, allows virtually all optical transitions, yielding an a-Si:H film absorption coefficient 10-fold higher than that of c-Si in the fluorescence wavelength region of commonly used dyes (500−650 nm, Figure 1).[25] Furthermore, the dark current of a-Si:H (~10^{-11} A/cm^2, 25 °C) is much lower than c-Si, facilitating low-noise detection. For these reasons, an a-Si:H photodiode is advantageous for the fabrication and operation of integrated detectors for microfluidic devices.

Here, we report the development and use of an a-Si:H PIN photodiode for fluorescence detection of separations performed with glass microfluidic CE devices. The properties of the a-Si:H photodiode are first explored using a conventional confocal optical system, demonstrating its ability to detect commonly used fluorescent dyes with high sensitivity. We then design and develop a hybrid integrated detection system comprised of a fluorescence collecting lens, a multilayer optical interference filter, and an annular a-Si:H PIN photodiode. This integrated system is characterized and used to detect DNA and amino acid separations.

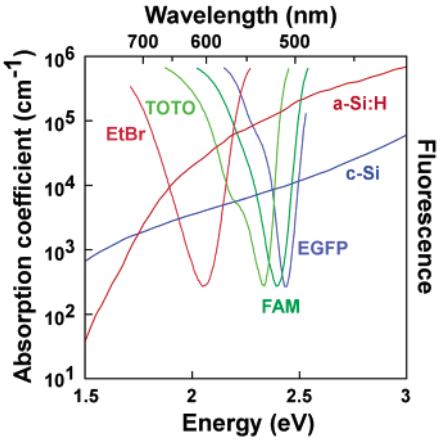

Figure 1. Absorption spectra of hydrogenated amorphous Si (a-Si:H, band gap ~1.7 eV) and single crystalline Si (c-Si, band gap 1.1 eV) with overlaid emission spectra of frequently used fluorescent dyes such as ethidium bromide (EtBr), TOTO, fluorescein (FAM), and enhanced green fluorescent protein (EGFP). Emission data are normalized.

EXPERIMENTAL SECTION

Microfluidic CE Fabrication. The microfluidic CE device was fabricated according to previously published procedures.[27] Briefly, Borofloat glass wafers (100 mm diameter, 1.1 mm thick, Precision Glass and Optics, Santa Ana, CA) were micromachined using HF wet chemical etching to produce channels 7.8 cm long × 50 μm deep × 120 μm wide for DNA fragment sizing and serpentine channels 21.4 cm long × 20 μm deep × 150 μm wide for amino acid analysis. Access holes were drilled for the sample, waste, cathode, and anode reservoirs, and the etched and drilled plate was then thermally bonded to a blank glass plate. Channel arms connecting the injection intersection with the sample, cathode, and waste reservoirs were 0.3, 0.4, and 0.3 cm in length, respectively, for the DNA analysis chip, and the channel arms were all 0.4 cm in length for the amino acid analysis chip.

a-Si:H Photodiode Fabrication. The a-Si:H PIN photodiode structure is shown in Figure 2. Chromium was sputtered on a Corning 1737 glass substrate (Precision Glass and Optics) at room temperature as the bottom electrode. This was followed by the deposition of P-doped (n layer, 100 nm thick), nondoped (i layer, 1 μm), and B-doped (p layer, 10 nm) a-Si:H films at 210−250 °C by plasma decomposition of SiH_4/PH_3, SiH_4, and SiH_4/B_2H_6, respectively (PECVD, ULVAC, Japan). Each layer was deposited in three separate chambers to avoid cross-contamination. Transparent indium tin oxide (ITO) was sputtered at room temperature as a top electrode. The outer diameter of the photodiode was 2.5 mm, and the pinhole diameter was 0.4 mm. The sidewall of the photodiode was covered by a plasma-deposited silicon nitride layer, followed by a sputtered Al layer. The Al layer on the outer

(16) Waters, L. C.; Jacobson, S. C.; Kroutchinina, N.; Khandurina, J.; Foote, R. S.; Ramsey, J. M. *Anal. Chem.* **1998**, *70*, 158−162.
(17) Paegel, B. M.; Yeung, S. H. I.; Mathies, R. A. *Anal. Chem.* **2002**, *74*, 5092−5098.
(18) Anderson, R. C.; Su, X.; Bogdan, G. J.; Fenton, J. *Nucleic Acids Res.* **2000**, *28*, e60.
(19) Burns, M. A.; Johnson, B. N.; Brahmasandra, S. N.; Handique, K.; Webster, J. R.; Krishnan, M.; Sammarco, T. S.; Man, P. M.; Jones, D.; Heldsinger, D.; Mastrangelo, C. H.; Burke, D. T. *Science* **1998**, *282*, 484−487.
(20) Roulet, J.-C.; Völkel, R.; Herzig, H. P.; Verpoorte, E.; de Rooij, N. F.; Dändliker, R. *Anal. Chem.* **2002**, *74*, 3400−3407.
(21) Chabinyc, M. L.; Chiu, D. T.; McDonald, J. C.; Stroock, A. D.; Christian, J. F.; Karger, A. M.; Whitesides, G. M. *Anal. Chem.* **2001**, *73*, 4491−4498.
(22) Yee, G. M.; Maluf, N. I.; Kovacs, G. T. A.; Hing, P. A.; Albin, M. *Sens. Actuators, A* **1997**, *58*, 61−66.
(23) Adams, M. L.; Enzelberger, M.; Quake, S. R.; Scherer, A. *Sens. Actuators, A* **2003**, *104*, 25−31.
(24) Webster, J. R.; Burns, M. A.; Burke, D. T.; Mastrangelo, C. H. *Anal. Chem.* **2001**, *73*, 1622−1626.
(25) *Technology and Applications of Amorphous Silicon*; Street, R. A., Ed.; Springer: New York, 2000.
(26) Sze, S. M. *Physics of Semicoductor Devices*; John Wiley & Sons: New York, 1981.
(27) Simpson, P. C.; Roach, D.; Woolley, A. T.; Thorsen, T.; Johnston, R.; Sensabaugh, G. F.; Mathies, R. A. *Proc. Natl. Acad. Sci. U.S.A.* **1998**, *95*, 2256−2261.

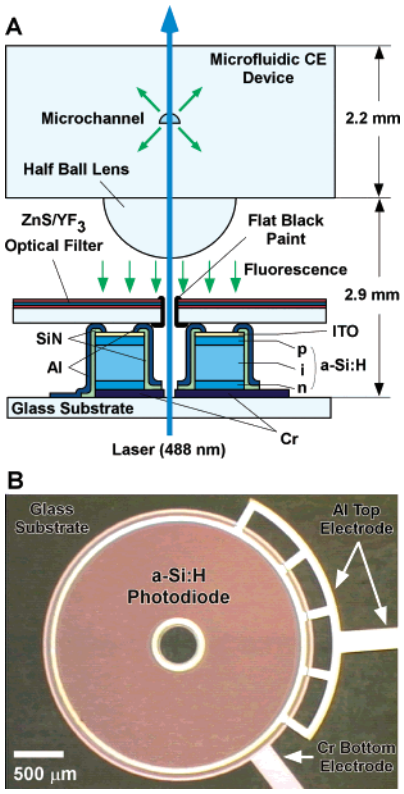

Figure 2. (A) Schematic cross-sectional view of the hybrid integrated a-Si:H fluorescence detector with a microfluidic electrophoresis device. (B) Optical micrograph of the top view of the annular a-Si:H photodiode.

wall makes contact with the ITO top layer, while the inner wall coverage prevents laser light scattering from reaching the photodiode. The discrete a-Si:H photodiode (active area: 1 × 1 mm square) was fabricated in the same way. The details of the a-Si:H photodiode fabrication were published previously.[25]

DNA Sample Preparation and Separation. For DNA separations, hydroxyethylcellulose (HEC, M_w = 438 kDa, Hercules, Wilmington, DE) dissolved in 1× Tris/acetate/EDTA buffer (TAE; 50 mM Tris base, 50 mM acetate, 1 mM EDTA) to 0.75% w/v was used as the sieving matrix. Oxyazole yellow (YO; Molecular Probes, Eugene, OR) was diluted to 1 μM concentration in the sieving matrix, and the mixture was degassed under vacuum with stirring for 5 min. The degassed mixture was centrifuged to remove particles and bubbles. The channels were coated with linear polyacrylamide in order to suppress electro-osmotic flow (EOF) and to prevent adsorption of DNA.[28] The entire channel was filled with the degassed HEC solution from the anode access hole using a 1-cc syringe. A *Hae*III digest of ϕX174 bacteriophage DNA ladder was diluted with water to 100 ng/μL, resulting in a solution with 2 mM Tris-HCl and 0.2 mM EDTA. The DNA sample was placed in the sample reservoir, and 1× TAE buffer was placed in the waste, cathode, and anode reservoirs to make electrical contact with the platinum electrodes. The DNA sample was injected for 30 s from the sample (100 V) to the waste reservoirs (500 V) while applying a pinching potential of 250 V at the cathode and anode reservoirs. The separation was then performed with 0 V at the cathode and either 1000 or 2000 V at the anode reservoir while applying 80 or 150 V back-biasing potential at the sample and waste reservoirs. The effective separation length was ~4 cm.

Amino Acid Sample Preparation and Separation. Amino acids were fluorescently labeled by adding 46 μL aqueous racemic glutamic acid (1 mM) to 49 μL of a fluorescein isothiocyanate (FITC, 1 mM in acetone with 0.1% v/v pyridine) labeling solution. The labeling reaction was buffered to pH = 10 by adding 5 μL of 200 mM sodium carbonate and incubated in the dark at room temperature for ~12 h. The reaction products were diluted 1/10 with running buffer (10 mM carbonate, 12 mM sodium dodecyl sulfate (SDS), pH 10). The final concentration of the derivatized glutamic acid was 23 μM both for D- and L-Glu. Enantiomeric resolution of the D- and L-isomers of glutamic acid was achieved by including a chirally discriminating γ-cyclodextrin (γ-CD; Sigma, St. Louis, MO) in the running buffer.[29,30] Before performing CE analysis, the channels were flushed for 1 h with 1 M NaOH followed by a deionized water rinse to achieve reproducible EOF. Separation and injection cross channels were filled with the running buffer using vacuum. The sample was then placed in the sample reservoir and loaded from sample (0 V) to waste reservoir (−1700 V) using a 20-s pinched injection (anode, −700; cathode, 0 V). Subsequently, separation potentials of 0 V at the anode and −12 500 V at the cathode were applied to separate the glutamic acid stereoisomers while back-biasing the sample and waste reservoirs (−500 V). The effective separation length was ~19 cm.

Detection System and Data Acquisition. The confocal fluorescence detection system used to evaluate the discrete a-Si:H photodiode is shown in Figure 3. Light from an argon ion laser (Ar^+, 488 nm) was focused on the separation channel through a microscope objective (32×, NA 0.4, Zeiss, Germany) to excite the fluorophore. Fluorescence gathered by the objective lens was spectrally filtered with a 60-nm band-pass filter centered at 535 nm (HQ535/60, Chroma, Brattleboro, VT) and spatially filtered through a 1-mm pinhole (Melles Griot, Carlsbad, CA) before being focused on the a-Si:H photodiode active area (1 mm^2). Electrical contacts were made with contact pads on the a-Si:H photodiodes using micromanipulators with metal needle probes (Rucker & Kolls, Milpitas, CA).

The design of the hybrid integrated a-Si:H detection system for microfluidic CE analysis is shown in Figure 2. A half-ball lens (2-mm diameter), a ZnS/YF_3 multilayer long-pass optical interference filter (E512LP, Chroma Technology) with a 250-μm-diameter drilled pinhole, and an annular a-Si:H photodiode were assembled and supported by a black anodized aluminum base, forming a compact platform for attachment to a microfluidic CE device. The half-ball lens was first glued to the aluminum housing, and laser light was directed normal to the ball lens and through its center. The optical interference filter was then aligned and glued such that the laser light passed centrally through its pinhole. The a-Si:H photodiode was placed 2.9 mm away from the external surface of the microfluidic CE device, and the total thickness of the integrated platform was only 3.6 mm. The a-Si:H photodiode was affixed to the filter plate to prevent scattered laser light from entering the photodiode. The microfluidic CE device was optically coupled to the integrated detector platform with index-matching fluid (Series A, n = 1.474, Cargille Laboratory, Cedar Grove, NJ).

(28) Hjerten, S. *J. Chromatogr.* **1985**, *347*, 191−198.
(29) Vespalec, R.; Bocek, P. *Chem. Rev.* **2000**, *100*, 3715−3753.
(30) Hutt, L. D.; Glavin, D. P.; Bada, J. L.; Mathies, R. A. *Anal. Chem.* **1999**, *71*, 4000−4006.

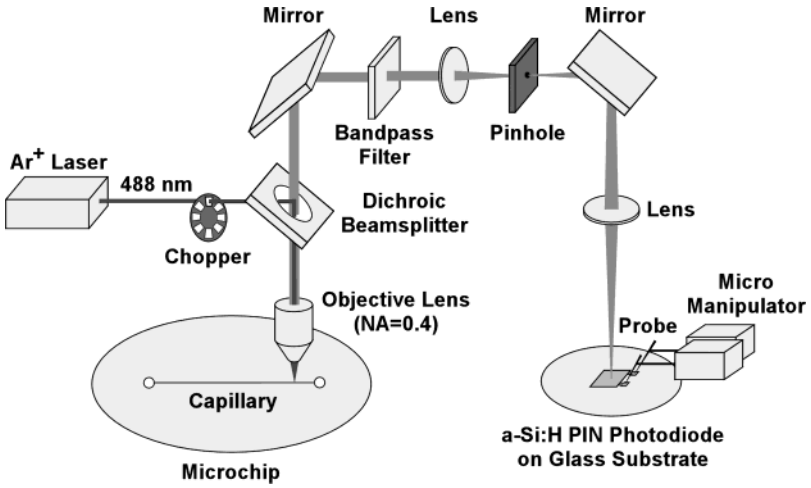

Figure 3. Laser-induced confocal fluorescence system using a discrete a-Si:H PIN photodiode to detect fluorescence from a microfluidic channel.

Laser light (488 nm) was introduced normal to the microfluidic CE device through the detector while loosely focused (~30 μm diameter) through a convex lens (NA ~0.01, focal length = 500 mm) on the CE channel. The annular a-Si:H photodiode and transparent glass substrate allowed vertical laser excitation while avoiding direct incidence of excitation light on the photodiode. The bottom 100-nm-thick Cr electrode layer of the a-Si:H photodiode acted as an aperture for the incident laser light. The filter pinhole was coated with flat black paint (blot diameter ~1.2 mm) to minimize laser light scattering. Fluorescence was collected by the half-ball lens and transmitted by the interference filter, which eliminated the excitation light. Ray trace simulation (ZEMAX, Focus Software, San Diego, CA) indicated that a 2-mm-diameter half-ball lens would approximately collimate the fluorescence emitted from a microchannel located behind the 1.1-mm-thick Borofloat substrate. Electrical contacts at the contact pads of the a-Si:H diode were made with copper leads using conductive epoxy.

For either the discrete or hybrid integrated detector, a reverse bias voltage of 1 V was applied to the a-Si:H photodiode to optimize carrier collection efficiency. The photocurrent was synchronized to chopped laser light at 27 Hz and detected by a lock-in amplifier (LIA; SR830, Stanford Research System, Sunnyvale, CA) to reduce background due to environmental light and dark current of the a-Si:H detector. The filtered (300 ms) LIA output was digitized at 20 Hz. Data acquisition and separation control were accomplished using LabView (NI-DAQ 1200, National Instruments, Austin, TX).

RESULTS AND DISCUSSION

A conventional confocal optical system was first used to characterize the a-Si:H PIN photodiode response to fluorescence under ideal optical conditions. A fluorescein solution was flowed in a 50-μm-deep channel at a constant rate of 800 μm/s, which is comparable to the velocity of small DNA fragments under typical CE conditions. Figure 4 presents the dependence of the fluorescence signal from the confocal a-Si:H PIN photodiode on fluorescein concentration (laser power, 1 mW). The fluorescence intensity increased linearly with fluorescein concentration (slope, 0.97 ± 0.01), and the limit of detection (LOD, $S/N = 3$) was 680 pM. The background signal measured from a buffer-filled channel was negligible (<100 fA) for a laser power of 1 mW. Shot noise

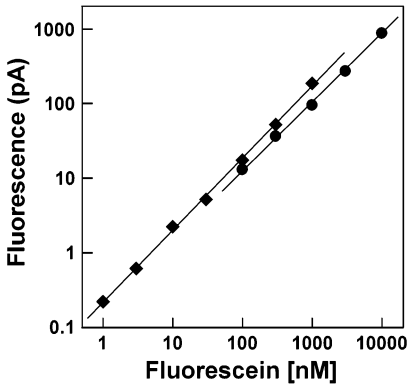

Figure 4. Lock-in amplified fluorescence signal from the discrete (◆ 1 mW laser power) and hybrid integrated (● 0.12 mW laser power) a-Si:H detectors plotted versus fluorescein concentration. The least-squares lines exhibit slopes of 0.97 ± 0.01 and 0.90 ± 0.02 for the discrete and integrated detectors, respectively. The buffer-only background of 430 pA has been subtracted in the case of the integrated detector, while no background signal was observed using confocal optics. The fluorescein solution in 1× TAE buffer was flowed through a 50-μm-deep channel at a constant flow rate of 800 μm/s.

of the a-Si:H photodiode is expected to be the dominant noise source in the lower photocurrent range; however, flicker noise (e.g., fluctuation in laser intensity and/or photodiode current) may contribute at higher fluorescein concentrations.

With the detector suitability confirmed, we designed and characterized a hybrid integrated a-Si:H detector for microfluidic CE devices. The device design exploits the optical transparency of the glass substrate used in a-Si:H photodiode fabrication to combine an annular detector with vertical laser excitation through the detector glass substrate. This design is impossible to realize using a c-Si photodiode because the c-Si wafer is opaque to visible light. With this design, the background level measured from a buffer-filled channel is around ~430 pA for a laser power of 0.12 mW. Figure 4 shows the dependence of the background-subtracted integrated a-Si:H detector fluorescence signal on fluorescein concentration for a laser power of 0.12 mW. Acceptable linearity with fluorescein concentration is observed (slope, 0.90 ± 0.02). This sublinearity is most likely due to inadequacies

in the background subtraction; separate calibration experiments with neutral density filters demonstrated the linear optical response of the a-Si:H photodiode. With the same excitation power and fluorescein concentration, the fluorescence intensity from the integrated detector is a factor of 3 higher than that observed from the discrete confocal detector. This is primarily due to the 4-fold larger solid angle of the half-ball lens in the integrated detection system, compared to the conventional confocal microscope system. This observation illustrates a key advantage of the integrated detection system.

The LOD ($S/N = 3$) for the integrated a-Si:H detector was found to be 17 nM, limited primarily by noise in the background photocurrent. Since, in this case, the background photocurrent is large, flicker noise may be the major noise source. The LOD for the hybrid integrated a-Si:H detector is ~20-fold higher than that for the discrete confocal a-Si:H detector, but it is comparable to the reported sensitivity of an integrated μAPD detector.[21]

The background (430 pA) photocurrent noise which determines the LOD of our hybrid integrated detectors arises primarily from specular laser scattering. About 100 pA out of the total background photocurrent is due to the presence of the microfluidic CE device, which may arise partly from Raman scattering of water. Possible causes of the specular scattering include the non-AR-coated surface of the ball lens and the sidewall of the optical filter pinhole coupled with the low optical density (~3.8) of the long-pass filter at 488 nm. The last point is particularly relevant in comparison with the confocal setup, in which a dichroic beam splitter is used to block the scattered laser light in addition to the interference filter. Improved filtering of the scattered light and/or AR coating of the components should lower the background and improve the LOD.

Figure 5 presents the separation and detection of a ϕX174 *Hae*III DNA digest ladder using the hybrid integrated a-Si:H detector. All 11 peaks of the DNA ladder are successfully detected with good S/N at both 130 and 260 V/cm. The detection limits ($S/N = 3$) for each fragment are ~500 pg/μL. For the higher separation field, 50 000, 40 000, and 70 000 theoretical plates are achieved for the 194, 234, and 603 bp fragments, respectively. Although better separations have been presented with conventional detection systems, the resolution is still much better than the DNA separation efficiency reported previously using an integrated c-Si photodiode detector.[24] The resolution was limited by the relatively high LIA time constant of 300 ms; decreasing the time constant to 100 ms allowed better resolution of the 271-, 281-, and 872-bp peaks. The separation efficiency can also be improved by decreasing the separation field, as shown in the lower electropherogram of Figure 5. In this case, the theoretical plate values are improved to 70 000, 70 000, and 100 000 for the 194-, 234-, and 603-bp fragments, respectively. These results demonstrate that integrating the a-Si:H detector with a microfluidic CE device provides the necessary sensitivity and separation efficiency for point-of-care clinical, genetic, and pathogen analysis.[31] By coupling our integrated a-Si:H detector with a microfluidic PCR–CE system,[15] it should be possible to develop a fully integrated, portable genetic analyzer with high speed, specificity, and sensitivity.

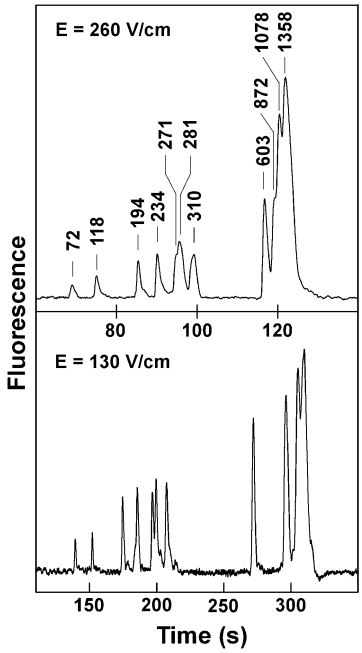

Figure 5. Analysis of a *Hae*III digest of ϕX174 bacteriophage DNA (100 ng/μL) using the integrated a-Si:H detector. The separation channel was 7.8 cm long, 120 μm wide, and 50 μm deep with an effective length of 4 cm. Hydroxyethylcellulose (HEC; 0.75 w/v%, M_w = 438 kDa) dissolved in 1× TAE buffer was used as the sieving matrix, and the separation was performed at 130 and 260 V/cm. On-column fluorescent labeling was accomplished with the DNA intercalating dye oxyazole yellow (YO, 1 μM). Theoretical plates achieved for the 194, 234, and 603 bp fragments are 50 000, 40 000, and 70 000 for the higher separation field and 70 000, 70 000, and 100 000 for the lower field, respectively.

The integrated a-Si:H detector will also be valuable in the development of portable, in situ chemical analysis devices. Specifically, we are working toward the use of this a-Si:H technology for biosignature detection in extraterrestrial environments such as Mars. Assuming that biogenic amino acids are homochiral, an enantiomeric excess of any given amino acid may confirm the presence of extinct or extant extraterrestrial life.[32] While it is reported that the Martian meteorite ALH84001 indicates biogenic activity on Mars,[33] the result remains controversial due to terrestrial contamination issues.[34] In situ analysis on Mars is required to eliminate such ambiguities.[30] Microfluidic analysis systems incorporating high-sensitivity integrated detection will be imperative for the success of these missions.

Based on this motivation, the hybrid integrated a-Si:H detector together with a microfluidic CE device was used to analyze a glutamic acid mixture labeled with FITC. Figure 6A presents a single peak characteristic of a glutamic acid separation in an achiral buffer (pH 10). Figure 6B shows that the D- and L-enantiomers are well resolved with excellent S/N when the buffer contains the chiral resolution agent γ-CD ($S/N = 36$ for D-Glu; 39 for L-Glu). The peaks are sufficiently sharp to provide a nearly baseline-resolved chiral separation (resolution = 1.35). In addition

(31) Kimura, R.; Mandrell, R. E.; Galland, J. C.; Hyatt, D.; Riley, L. W. *Appl. Environ. Microbiol.* **2000**, *66*, 2513–2519.

(32) Bada, J. L. *Nature* **1995**, *374*, 594–595.

(33) McKay, D. S.; Gibson, E. K.; Thomas-Keprta, K. L.; Vali, H.; Romanek, C. S.; Clemett, S. J.; Chillier, X. D. F.; Maechling, C. R.; Zare, R. N. *Science* **1996**, *273*, 924–930.

(34) Bada, J. L.; Glavin, D. P.; McDonald, G. D.; Becker, L. *Science* **1998**, *279*, 362–365.

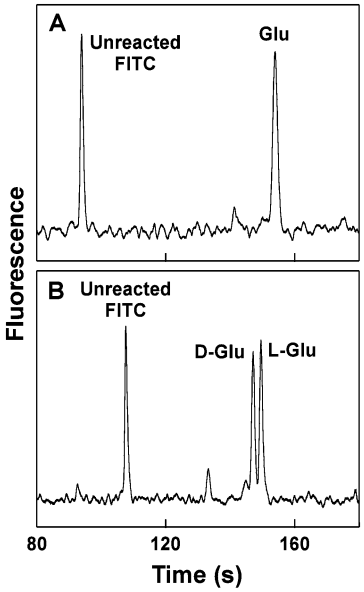

Figure 6. Separation and detection of fluorescein-labeled glutamic acid with the integrated a-Si:H detector. The concentration of the derivatized glutamic acid was 23 μM for both the D- and L-isomers. (A) Achiral separation of Glu without γ-CD in the running buffer. (B) Chiral separation of Glu enantiomers with 40 mM γ-CD in the running buffer. The 21.4-cm-long serpentine channel had an effective channel length of ~19 cm. Running conditions: carbonate buffer (10 mM Na_2CO_3, 12 mM sodium dodecyl sulfate), separation field 600 V/cm.

to its robust integrated construction, the radiation hardness of the a-Si:H photodiode[35] makes it ideal for performing amino acid composition and chirality analyses in harsh extraterrestrial environments. Despite the proximity of the detector to the high-potential CE channel, electrical perturbation of the a-Si:H photodiode did not occur. The top ITO contact layer of the a-Si:H PIN photodiode effectively isolates the diode from the CE electrical potential.

In summary, we have demonstrated the suitability of using a-Si:H photodiodes for fluorescence detection as well as a hybrid integrated optical detector for microfluidic CE devices. DNA analysis experiments establish clinically relevant limits of detection for point-of-care genetic analysis, and enantiomeric analysis experiments demonstrate the potential of this technology to address the needs of remote extraterrestrial biosignature detection apparatus. In the present device, an a-Si:H photodiode, an optical filter, and a microlens were manually assembled. The ZnS/YF_3 filter, however, can be monolithically integrated on the a-Si:H photodiode, which can withstand the filter coating temperature (~100 °C), by inserting an intermediate layer of SiN or SiO to prevent the diffusion of filter elements into the a-Si:H photodiode. Additionally, microlens arrays[20,36] and a-Si:H sensor arrays[25] have been demonstrated, so it should be possible to fabricate a detachable, compact, reusable detection unit that integrates a dense array of microlenses, optical filters, and a-Si:H detectors for highly parallel microfluidic assays. From the viewpoint of laser integration, an important aspect of the present device is vertical laser excitation through the detector. When combined with vertical cavity surface emitting laser (VCSEL) diodes,[37] the current integrated a-Si:H detector should facilitate the construction of coaxial excitation-detection modules for applications as diverse as point-of-care clinical genetic and pathogen analysis, biological warfare detection, and in situ remote chemical analysis. The extension to a-Si:H−VCSEL-based excitation-detection arrays may play an important role in emerging large-scale integrated microfluidic devices.

ACKNOWLEDGMENT

The authors gratefully acknowledge microfluidic chip fabrication by Stephanie Yeung and a-Si:H photodiode fabrication by the process line at the Palo Alto Research Center. Microfluidic chip fabrication was carried out at the University of California, Berkeley Microfabrication Laboratory. This research was supported by grants from the National Institutes of Health (HG01399) and from the Director, Office of Science, Office of Biological and Environmental Research of the U.S. Department of Energy under Contract (DE-FG03-91ER61125). T.K. was supported by a Japan Science and Technology Corporation overseas fellowship (JST99108).

Received for review April 21, 2003. Accepted July 11, 2003.

AC0301550

(35) Kagan, M.; Nadorov, V.; Guha, S.; Yang, J.; Banerjee, A. *IEEE PVSC Proc.* **2000**, 1261−1264.
(36) Hutley, M. C. *Refractive Microlens Arrays*; Taylor & Francis: London, 1997.
(37) Iga, K. *IEEE J. Sel. Top. Quantum Electron.* **2000**, *6*, 1201−1215.